IMM
DEPARTMENT OF MATHEMATICAL MODELLING

Technical University of Denmark
DK-2800 Lyngby – Denmark

J. No. x585
1996-12-6
LHH

DYNAMIC ANALYSIS OF A LOW ENERGY TEST HOUSE AND A CENTRAL HEATING SYSTEM

Lars Henrik Hansen

TECHNICAL REPORT
IMM-REP-1996-20

IMM

GRUNDFOS®

ISBN SIDE

Abstract

This report is concerned with the description and the modelling of the heat transfer in a test house at the Department of Buildings and Energy (IBE) at the Technical University of Denmark (DTU). The test house is a single-storeyed low energy house and it is fairly well known due to some previously performed experiments. A water based central heating system is used as heating system. The report presents the preliminary analysis of the heat dynamics in the test house and the central heating system with respect to a succeeding house heating experiment. Input sequences to the water based central heating system are designed.

Lyngby, December 6th 1996.

Keywords

Heat dynamics; Low energy house; Non-linear system; Input design

Contents

1 Introduction

1.1 Background

The prospects of a successful experiment are strongly correlated with the preliminary investigation and analysis of the experiment. A profound investigation and analysis is especially important, if the experiment takes long time, or if, it for some reason, is difficult to repeat.

The experimental setup discussed in this report consists, in short terms, of a low energy test house at the Department of Buildings and Energy (IBE) placed in the northern campus area of the Technical University of Denmark (DTU) (see *(Rasmussen and Saxhof, 1982)*), and of a water based central heating system – designed by the author and built by Grundfos A/S in the autumn of 1995. The purpose of the experiment is to model/identify the heat transfer process from the central heating unit, through the heating system and through the house to the ambient of the test house. Due to the big time constants in a house, the duration of such an experiment will be long (e.g. three weeks), and as the experimental boundaries consist of the clima (i.e. sun, wind and ambient temperatures), the experiment cannot be repeated. The experiment is to succeed this report.

One way to analyse an experimental setup is to establish a model of the dynamic properties in the experiment. This model can then be used to predict or to simulate the heat transfer based on certain conditions.

The heat transfer experiment has two kinds of input:

1. controllable inputs, e.g. pump speed or water supply temperature.
2. climatic inputs, e.g. solar radiation, ambient air temperature which are non-controllable inputs.

Given a set of climatic inputs, it might be possible to define a set of controllable inputs that, together with the climatic inputs can ensure an adequate level of information in the experiment. The most used type of controllable inputs are the so called PRBS (Pseudo-Random Binary Signals, see *(Godfrey, 1980)*).

In this report the modelling of the experimental setup is based on *prior* knowledge, i.e. physical knowledge, available data and results obtained in previous experiments, see e.g. *(Rasmussen and Saxhof, 1982)*, *(Hansen, 1985)*, *(Madsen et al., 1990)*.

1.2 Outlines of the report

In the next section the water based central heating system, the low energy test house and the data acquisition equipment are described.

Section 3 deals with the modelling of the heat transfer processes in the experiment.

In Section 4 the design of the controllable inputs is described.

Finally a summarising section with discussion is given.

2 The experimental setup

In this section the experimental setup is described. The description is divided into three parts, i.e. a description of:

1. Water based central heating system.
2. Test house.
3. Data acquisition system.

The test house is divided into two general zones: 1) a test zone with the heat network (radiators, valves, etc.) and 2) a control zone containing the heating unit, the data acquisition PC, etc.

2.1 The central heating system

A water based central heating system is used as heat installation in the test house. The central heating system was designed by the author and built by Grundfos in the autumn of 1995. It consists of a heating unit and of two radiator terminals. The central heat system is configured as a 2-string network (see Figure 1).

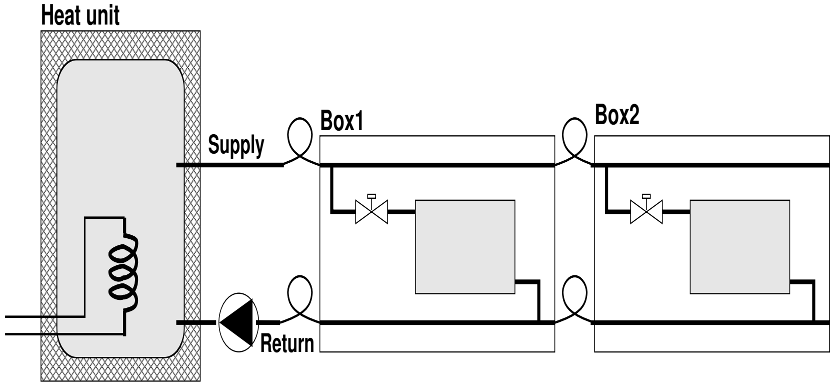

Figure 1: *Sketch of the central heating system, consisting of a heating unit and two radiator terminals, which are configured as a 2-string network.*

The design of the central heating system was governed by two criteria:

1. It should fit the heat consumption of the test house.
2. It should be easy to move the central heat system in and out of the test house.

The two posed criteria have implied special demands to the design. The resulting central heating system is configured in three movable units, i.e. one heat unit and two radiator units.

The heating unit is based on a 80 litters tank. The heat source is a 2.5 KW electric heat element, which is on/off controlled by an E5AJ controller (Omron). The set point of the heating unit temperature (the supply temperature) can be set to a valve between 0 °C – 100 °C , either locally or remote by data acquisition equipment. An UPE25-60 180 pump (Grundfos) is placed in the return pipe of the heat network. The speed of the pump is remote controlled by a 0–5 V signal from the data acquisition equipment. Thereby, the dynamic pressure in the heating system can be changed from approximately 0.1 to 6.0 mWc (depending on the flow). A sketch of the heating

unit is shown in Figure 2.

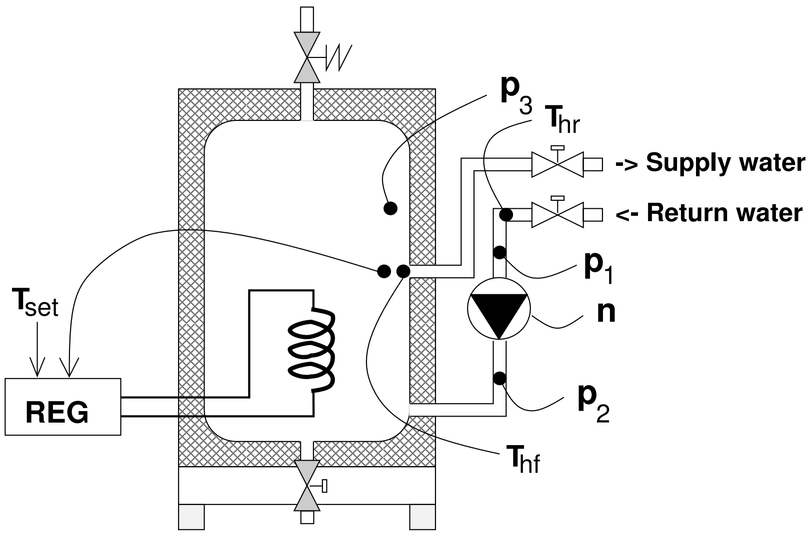

Figure 2: *Sketch of the heating unit.*

The two radiator units are identically. Each radiator has a nominal power of 395 W. Dimensions are: 0.3 m × 0.6 m (height × length) – approximately 5 litters. A RA-FN 15 (Danfoss) thermostatic valve is placed in the inlet to the radiator. The valve/radiator arrangement is placed inside of a box with removable top, bottom and front wall, as indicated in Figure 3. The box frame is based on non-massive iron uprights. The wall is a sandwich construction consisting of a 3 mm iron plate (outer side), 75 mm of mineral wool (the middle) and a 1 mm lattice[1] aluminium plate (inner side). The volume of the closed box is approximative 0.5 m^3.

Two 150 W peltier elements are built into the top and front wall, respectively. The peltier elements can be used to cool the box when it is closed. In the succeeding test house experiment the box will be used in the open configuration.

[1] with approximately 40 % perforation

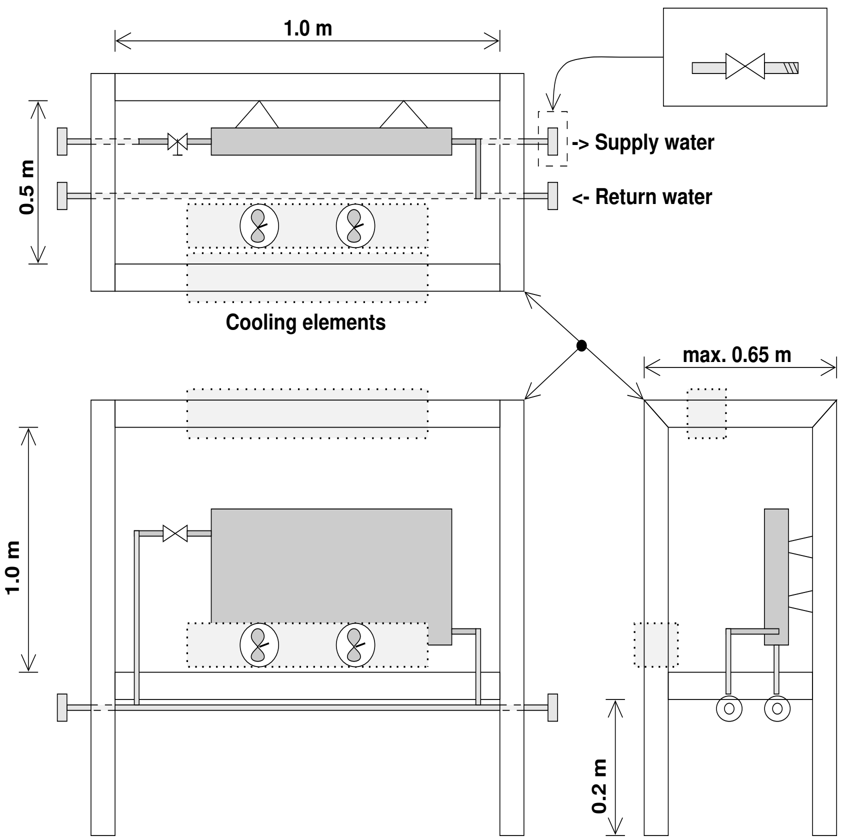

Figure 3: *Sketch of the radiator box unit, seen from the top, the front and the right hand side. The top, front and bottom walls can be removed. Furthermore, the top and front wall each contain cooling elements.*

2.2 The test house

The low energy test house is a single-storeyed building with a non-ventilated crawl space and a roof space used as office space. It was built around 1980, and it is located in the northern part of the campus area (Building 121A). The term *low energy* refers to nominal heat consumption, which is about 2.5 KW at -12 °C outside and 20 °C inside (i.e. a nominal heat loss of ∼78 W/°C).

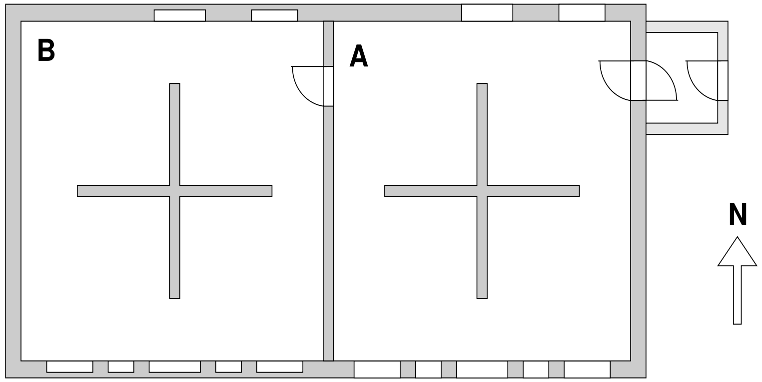

Figure 4: *A sketch of the test house ground plan.*

The ground floor of the test house conforms a test area of 120 m^2. As sketched in Figure 4, the ground floor is divided into two equal sized rooms (each of 60 m^2) by a wall insulated with 95 mm mineral wool. The west room is denoted by a "B", and the east room by "A". Furthermore, each room is partly separated into four smaller rooms by a cross wall in the middle of the room (see Figure 4). The outer wall and the ceiling of the ground floor are light sandwich constructions based on a masonite beam insulated with 300 mm mineral wool. The window area in room A makes up 25 % of the A room floor area – 16 % facing south. The windows in room B are identical to those in room A, except that the windows in room B are shielded. All the windows are triple glassed. The test house is extremely tight.

The floors in room A and B are layer constructions. From the bottom the floor in room A consists of: 22 mm plywood, 300 mm mineral wool, 22 mm plywood, and 75 mm concrete, while the floor in room B consists of: 22 mm plywood, 300 mm mineral wool, 22 mm plywood, 50 mm polystyrene, and 22 mm chipboard. This makes room A thermally more heavy than room B. Meanwhile, the floor in room B is (almost) covered with a double layer of concrete flags, each flag with area 0.16 m^2 and thickness 50 mm. Thus, the thermal heat capacity of room B should be about the same as the thermal heat capacity of room A.

The test house is divided into two zones, room A as the test zone and room B as the control zone, in order to have well defined experimental conditions. The heating unit (denoted "HU") is placed in room B, as shown in Figure 5. In order to separate the two radiator terminals, room A is divided into a northern and southern oriented room by the two cross patterned walls, as indicated in Figure 5. The two new rooms are denoted by "room An" and "room As", respectively. "n" and "s" refer to the northern and southern orientation, respectively. Hence, a radiator terminal (denoted e.g. "Box 1", see Figure 5) is placed in each of the A-rooms. Insulated cast-iron pipes are used in the heating unit and in the radiator terminal constructions. The heat distribution pipes, connecting the heating unit with the two radiator terminals, consist of insulated rubber/plastic tubes.

An additional heat input is placed in room An (denoted "EC" in Figure 5). The EC-unit is also remote controlled, i.e. a 0-5 V on/off signal could control an electrical on/off heat input of 0 or 150 W. The idea of the "EC"[2] will be discussed in Section 4.2.

2.3 Data acquisition system

The data acquisition system consists of pressure, flow, temperature, light and wind sensors, converter equipment and a computer, which is used to acquire and store the measured data. The heart of the acquisition system is a acquisition computer (denoted PC-unit). It is placed next to the heating unit, as indicated in Figure 5. To get an overview of the acquisition system and the measured quantities, the description is divided into: the central

[2]abbreviation of: electric cooker

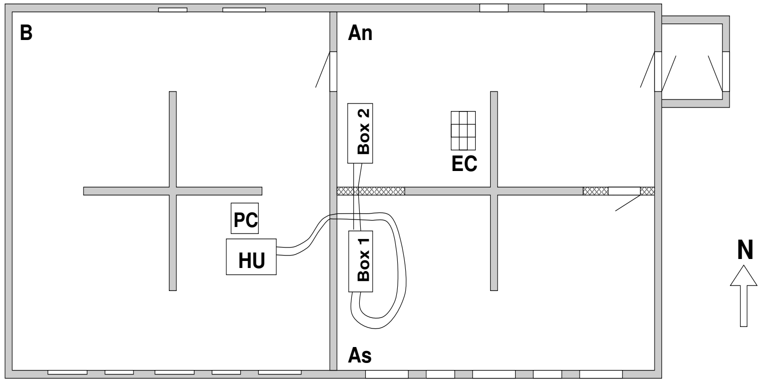

Figure 5: *The heat installation. The heating unit is denoted by "HU" and the two radiator terminals by "Box1" and "Box2", respectively. Insulated tubes are used as connecting pipes.*

heating system, the test house and the PC-unit.

2.3.1 Acquired central heating system quantities

The quantities acquired in the central heating system are pressures, flows and temperatures. In connection with the heating unit, the pressure over the pump, the pressure in the tank, the tank temperature (alias the supply temperature) and the return temperature are measured, as shown in Figure 2. Furthermore, the pump speed and the set point of the supply temperature are controlled from the PC-unit as described in Section 4.

In each of the radiator terminal the flow, the pressure before the valve, the pressure between the valve and the radiator, the pressure after the radiator, the inlet and outlet temperature and the air temperature next to the thermostatic valve are measured. Additionally, the surrounding air temperature is measured at the upper outer edge of the box, see Figure 6 (opposite end of the thermostatic valve measurement).

Hence, all in all, 21 quantities are measured, distributed as: 9 pressures, 2

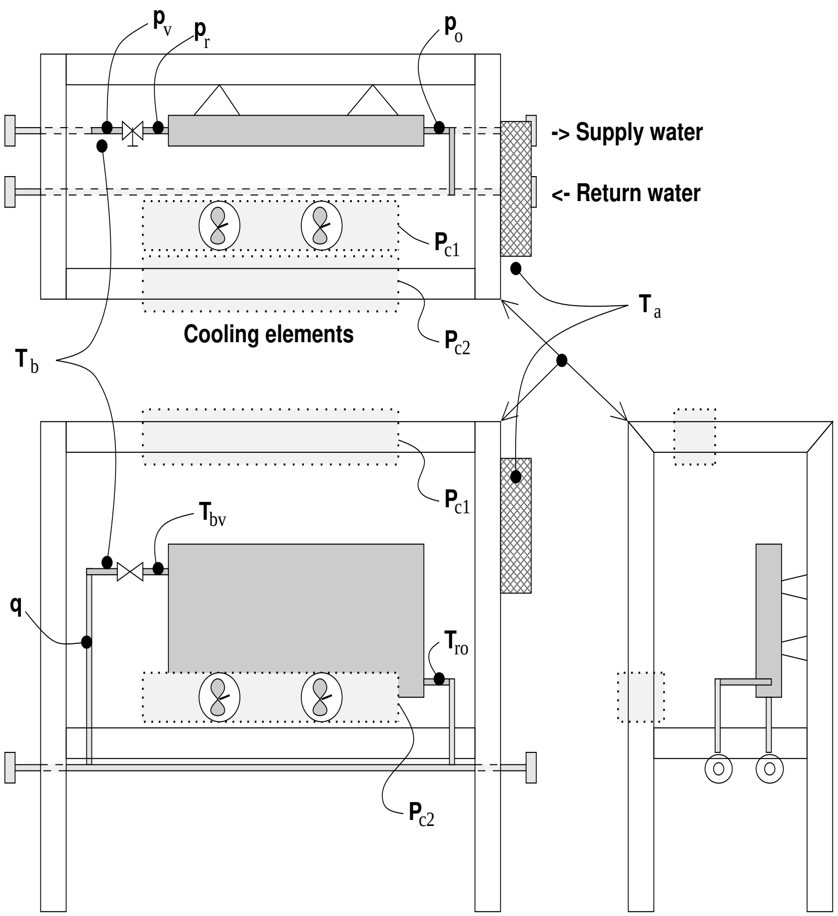

Figure 6: *Measured heating unit quantities.*

flows, 6 water temperatures and 4 air temperatures.

2.3.2 Acquired test house quantities

The acquired test house quantities are air temperature, solar radiation and wind speed. As described before the test house is divided into two zones. Two air temperatures, T_{bn} and T_{bs}, are measured in the control zone. Four air temperature, T_{nw}, T_{ne}, T_{sw} and T_{se}, are measured in the test zone, two in each of the test rooms. As sketched in Figure 7, the norther and southern ambient temperature are measured together with the horizontal solar radiations, north and south, respectively. The wind speed is also measured.

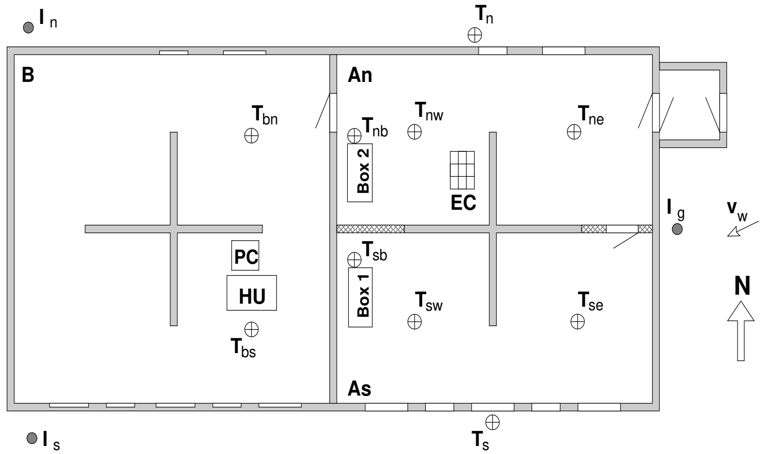

Figure 7: *Measured thermal quantities. NB. v_w is measured approximately 5 m over the house roof.*

The temperature measurements in the test house are based on the thermocouples (type T). The thermocouple signals are converted into suitable electric temperature signal by 6B11 modules (Analog Devices).

The measurements of the solar radiation are based on two vertical measurements – I_n to the north and I_s to the south – and one global measurement on the top of the roof. Additionally, the wind speed is measured 5 m over the top of the roof.

Hence, all in all, 12 quantities are measured, distributed as: 8 air temperatures, 3 solar radiations and one wind speed.

2.3.3 The PC-unit

The heart of the data acquisition system is a 75 MHz Pentium computer with 16 Mb memory and 1 Gb disc space. The data acquisition is based on a DT 3003 board (Data Translation) and on 8 6B11 modules (Analog Devices). The DT 3003 board has 32 differential or 64 single ended input channels (analog to digital), two analog output channels (digital to analog), 8 digital input/output lines and one counter/timer unit. The resolution of both input and output signals is 12 bits. The 8 6B11 modules are used to convert 8 thermocouple signals. The converted data are accessed from the acquisition computer through serial communication on port A. A sketch of the main part of the data acquisition system is shown in Figure 8.

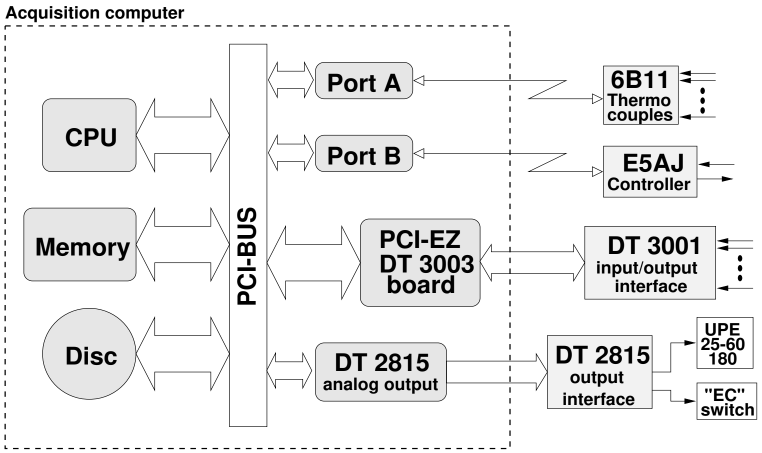

Figure 8: *The data acquisition system.*

The set point of the water supply temperature (the water tank temperature)

is controlled by the E5AJ controller (Omron). The set point is specified by the acquisition computer through serial communication on port B.

The DT 2815 board (Data Translation) has 8 (12 bits) digital to analog output channels. One of the channels is used to set the pump speed reference. Another channel is used to switch the EC-unit on and off.

As acquisition software DT VEE (Data Translation) is used. DT VEE is a visual programming software tool for data acquisition for Windows 3.1, see *(Data Translation, 1995)*. A data acquisition program has been customized to the system described above. The data acquisition program acquires and stores 33 signals and it controls three devices at a sample time of 10 seconds.

3 Modelling the experimental setup

This section describes the modelling of the experimental setup. The modelling is divided into: 1) modelling of the water based central heating system, and 2) modelling of the test house.

3.1 Model of the central heating system

An interesting modelling approach of the water based central heating system can be found in *(Aggerholm, 1983)*, where the basic idea is to describe the *static* relation between the pressure drops/losses and the flow in the pipe system.

3.1.1 Pipe model

The following modelling approach has previously been reported in *(Hansen et al., 1995)*, where the basic idea was to describe the *dynamic* relation between the pressure drops/losses and the flow in the pipe system. The basic element in the water based central heating system is the pipe.

The central heating system is viewed as an interconnected network of pipe elements, as sketched in Figure 9.

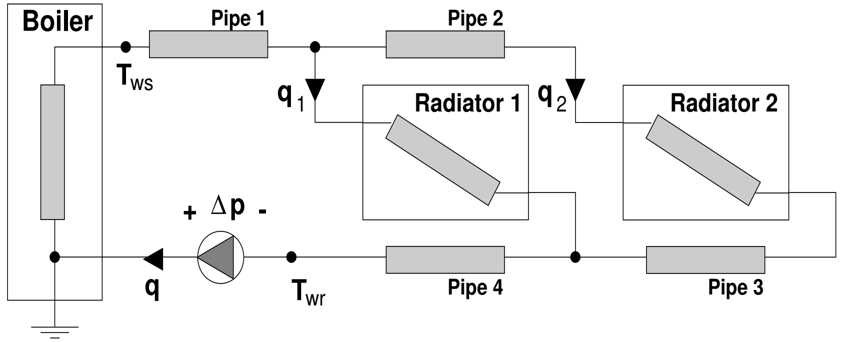

Figure 9: *Sketch of the water based central heating system. A lumped description using a parametric pipe modelling approach.*

In the following, the flow in the pipes, is assumed to be one dimensional. The flow can either be laminar or turbulent. Laminar flows occur at small velocities of the fluid (see *(Fox and McDonald, 1985; Zoebl and Kruschik, 1978)*), and an upper laminar flow limit can be distinguished using Reynolds number:

$$Re = \frac{v\,d}{\nu} \tag{1}$$

where v denotes the mean velocity of the flow, ν the kinematic viscosity of the fluid and d the inner diameter of the pipe. When $Re \leq 2300$ the flow is laminar.

What type of flow could actually be expected in the central heating system ? This question can be answered using (1). A typical pipe diameter of 15 mm at e.g. 60°C hot water ($\nu \approx 0.474 \cdot 10^{-6}$ m^2/s) yields the maximum laminar fluid velocity:

$$v_{max} = \frac{2300 \cdot 0.474 \cdot 10^{-6}}{0.015} \approx 73 \text{ mm/s} \tag{2}$$

which is equivalent to the maximum flow:

$$q_{max} = \frac{\pi}{4}(0.015)^2 v_{max} \approx 1.28 \cdot 10^{-5} \text{ m}^3\text{/s} \ = 46 \text{ l/h} \tag{3}$$

This flow must/should be compared with the *nominal radiator flow*, which will be explained later. The installed radiator power is $\Phi_0 = 395$ W at the supply/return/room-temperatures: 90°C /70°C /20°C (the standard conditions, see e.g. *(Johansen et al., 1979)*). The nominal flow for the installed radiator is:

$$q_0 = \frac{\Phi_0}{c_p q \Delta T} \approx \frac{395}{4200 \cdot 1000 \cdot (90 - 70)} \approx 17 \text{ l/h} \tag{4}$$

In the current configuration the maximum flow is approximately 90 l/h. Thus, both laminar and turbulent flow are possible flow states.

However, for simplicity the flow will first be considered to be laminar. A given flow q [m^3/sec] through a pipe will result in a corresponding pressure drop Δp [Pa] over the pipe in the down stream direction. This pressure drop occurs due to 1) the fluids friction against the pipe wall, and 2) viscous friction (internal fluid friction). Using dimension analysis (see *(Fox and McDonald, 1985)*), the pressure drop Δp_f due to friction can be modelled as:

$$\Delta p_f = \lambda \frac{l}{d} \frac{v^2}{2} \rho \tag{5}$$

where l denotes the length of the pipe, λ is the friction factor, and ρ denotes the density of the water. In the laminar case (see *(Fox and McDonald, 1985)*) the friction factor is given as $\lambda = \frac{64}{Re}$, which together with (1) and (5) yields:

$$\Delta p_f = 32 \frac{l \nu}{d^2} v \rho = R_l q \tag{6}$$

where $R_l = 32 \frac{l \nu \rho}{d^2 A}$ denotes the laminar hydraulic resistance. The pipe contains the water mass M, which leads to the introduction of inertia. Newton's second law together with the following two assumptions: 1) the cross sectional pressure drop at the input and the output of the pipe is uniform (one dimensional flow) and 2) the water is incompressible (i.e. $\frac{dM}{dt} = 0$), yield:

$$\frac{d(M\ v)}{dt} = \sum_i F_i \tag{7}$$

or

$$M\frac{dv}{dt} = p_{in}A - p_{out}A - F_f \tag{8}$$

where A denotes the sectional pipe area. The forces in the pipe are shown in Figure 10.

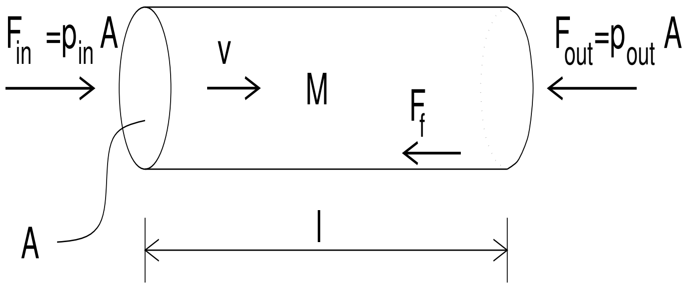

Figure 10: *Sketch of the pipe model.*

In a steady-state situation $\frac{dv}{dt} = 0$, hence:

$$F_f = p_{in}A - p_{out}A = \Delta p_f A = R_l q A \tag{9}$$

Using this result, together with the two relations: 1) $q = Av$, and 2) $M = \rho A l$, equation (8) can be rewritten as:

$$\frac{dq}{dt} = \frac{1}{L}(\Delta p - R_l q) \tag{10}$$

where $L = \frac{\rho l}{A}$, $R_l = 32\frac{l\nu\rho}{d^2A}$ and $\Delta p = p_{in} - p_{out}$. This first order differential equation describes the dynamic relation between the pressure drop over the pipe and flow in the pipe. Thus, in the laminar case the transfer function

from Δp to q can be written as:

$$\frac{Q_i(s)}{\Delta P(s)} = \frac{G}{\tau s + 1} \tag{11}$$

where

$$G = \frac{1}{R_l} = \frac{d^2A}{32l\nu\rho} \tag{12}$$

$$\tau = \frac{L}{R_l} = \frac{d^2}{32\nu} \tag{13}$$

An electrical equivalent to the laminar case is shown in Figure 11.

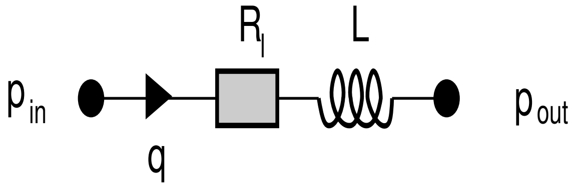

Figure 11: *Electrical equivalent of the laminar flow model.*

The "usual" way to model a pressure drop in the case of turbulent flow ($Re > 3000$, see *(Fox and McDonald, 1985)*), e.g. in a valve, is to use the quadratic relation:

$$\Delta p = K_v q^2 \tag{14}$$

According to *(Aggerholm, 1983)*, modelling the turbulent pressure drop using (14) might be a somewhat misguiding approximation – as exponents in the range of 1.51 to 2.16 have been reported in the literature. Hence, in this report, the turbulent pressure drop will be modelled as:

$$\Delta p = R_t q^k \tag{15}$$

where $R_t = \frac{\lambda l \rho}{2dA^k}$ denotes the turbulent hydraulic resistance. It should be noted that, R_t is a function of λ. Thus, the turbulent version of (10) is:

$$\frac{dq}{dt} = \frac{1}{L}(\Delta p - R_t q^k) \tag{16}$$

Furthermore it should be noted that, the friction factor λ, in the turbulent case, is given as an implicit expression (the Colebrook equation, see e.g. *(Fox and McDonald, 1985)*):

$$\frac{1}{\sqrt{\lambda}} = -2\log_{10}\left(\frac{2.51}{Re\sqrt{\lambda}} + \frac{e}{3.71 \cdot d}\right) \tag{17}$$

where e denotes the pipe roughness.

To get a more general description of the static relation between the pressure drop and the flow in a pipe, a "flow dependent" hydraulic resistance could be introduced:

$$\Delta p = R(q)q \tag{18}$$

where

$$R(q) = \begin{cases} R_l & \text{in the laminar case} \\ R_t|q|^{k-1} & \text{in the turbulent case} \end{cases} \tag{19}$$

With this formulation, it is possible to describe both equation (10) and (16) with one equation:

$$\frac{dq}{dt} = \frac{1}{L}(\Delta p - R(q)q) \tag{20}$$

As described in connection with (16), R_t is a function of λ, which further is dependent on Re. Hence, R_t is dependent on the flow q. For convenience, this dependency is neglected in the following calculation of the gain and the time constant in the case of turbulent flow. Thus, linearization of (16) yields:

$$G = \frac{1}{k\ R_t\ q_0^{k-1}} \tag{21}$$

$$\tau = \frac{L}{k\ R_t\ q_0^{k-1}} \tag{22}$$

where q_0 denotes the linearization flow.

What actually happens with the hydraulic resistance in the buffer zone (i.e. $Re \in [2300; 3000]$), when the flow changes from laminar to turbulent

flow (or vise versa), is still an open question. Would it be right to claim that $R_l \equiv R_t|q_{limit}|^{k-1}$, where q_{limit} is the limit flow between laminar and turbulent flow ?

3.1.2 Radiator model

From a hydraulic point of view, the radiator can be viewed as just a special pipe with a rectangular sectional area. As the derivation of (10) is based on the circular pipe geometry, an equivalent hydraulic diameter d_r of the radiator must be used (see *(Fox and McDonald, 1985)*), i.e.:

$$d_r = \frac{4A_r}{P_r} \tag{23}$$

where A_r denotes the sectional area of the radiator and P_r the perimeter of this sectional area. It can be verified that this definition includes the pipe geometry as a special case (i.e. $d_r = 2r$). The flow in a radiator is typically laminar due to a big[3] sectional area. Thus, using (23) in (10) implies that, (10) can cover other geometries than the circular pipes. The dominating hydraulic pressure drop in the radiator is related to the water entering the radiator, see *(Thor Eura, 1990)*.

Regarding the thermal properties of the radiator. The nominal radiator power Φ_0 is defined at the so called standard conditions. The standard conditions refer to $T_{i,0} = 90°\text{C}$ supply temperature (inlet to the radiator), $T_{o,0} = 70°\text{C}$ return temperature (outlet from the radiator) and $T_{a,0} = 20°\text{C}$ ambient temperature (the room temperature).

For convenience the following two mean temperature differences are introduced. The arithmetic mean temperature difference is defined as:

$$\Delta T_{ma} = \frac{T_i + T_o}{2} - T_a \tag{24}$$

[3] compared with the sectional area of a pipe

and the logarithmic mean temperature difference as:

$$\Delta T_{ml} = \frac{T_i - T_o}{\log_e\left(\frac{T_i - T_a}{T_o - T_a}\right)} \tag{25}$$

where $\log_e$ is the natural logarithm. At standard conditions $\Delta T_{ma,0} = 60$ °C and $\Delta T_{ml,0} = 59.4$ °C .

Two of the most common (static) thermal radiator models in the literature are the one and the two exponent formula. The one exponent formula is given as (see *(Weber, 1970; Becher, 1972)*):

$$\Phi = \Phi_0 \left(\frac{\Delta T_{ma}}{\Delta T_{ma,0}}\right)^{n_1} \tag{26}$$

where ΔT_{ma} denotes the actual arithmetic mean temperature difference, and $\Delta T_{ma,0}$ denotes the arithmetic mean temperature difference at standard conditions. The exponent n_1 is normally around 1.3.

The two exponent formula defined in (see *(Johansen et al., 1979)*) as:

$$\Phi = \Phi_0 \left(\frac{\Delta T_{m1}}{\Delta T_{m0}}\right)^{n_1} \left(\frac{\Delta T_{m2}}{\Delta T_{m1}}\right)^{n_2} \tag{27}$$

$$= \Phi_0 \left(\frac{\Delta T_{m1}}{\Delta T_{m0}}\right)^{n_1 - n_2} \left(\frac{\Delta T_{m2}}{\Delta T_{m0}}\right)^{n_2} \tag{28}$$

where ΔT_{m0} denotes the logarithmic mean temperature difference at standard conditions, ΔT_{m2} at actual mean temperature difference, and ΔT_{m1} denotes mean temperature difference at the actual supply temperature and at standard flow (see *(Johansen et al., 1979)*). The exponent n_1 is still around 1.3 and n_2 is in the area of 1.2 to 2.4 – dependent on the radiator type, see e.g. *(Johansen et al., 1979; Hallgreen and Paulsen, 1987)*. It should be noted that n_1 is related to constant flow and n_2 to constant supply temperature.

The definition of ΔT_{m1} is not straight forward. Therefore the following interpretation is used. As T_i the actual supply temperature is used. The

standard flow $q_0 \approx 17$ l/h was calculated in (4) for the installed radiators. Hence, at standard flow and at standard ambient temperature, the return temperature in ΔT_{m1} can recursively be calculated from:

$$\frac{\Phi}{\Phi_0} = \frac{c_p \rho q (T_i - T_o)}{c_p \rho q_0 (T_{i,0} - T_{o,0})} = \left(\frac{\Delta T_{m2}}{\Delta T_{m0}}\right)^{n_1} \tag{29}$$

In the data sheet on the used radiator Φ_0 is reported to 395 W, $n_1 = 1.25$ and $n_2 = 1.25$. As the two exponents are equal, the two exponent formula is reduced to:

$$\Phi = \Phi_0 \left(\frac{\Delta T_{m2}}{\Delta T_{m0}}\right)^{n_2} \tag{30}$$

A graphical illustration of the used radiator is shown in Figure 12.

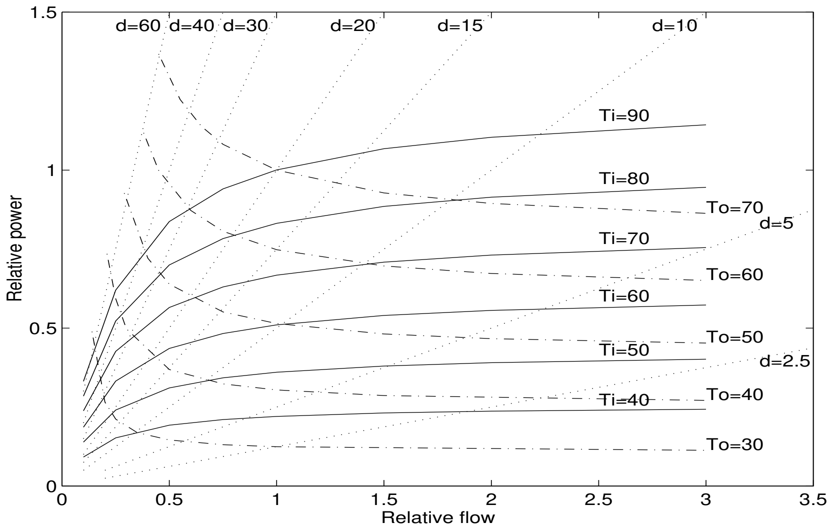

Figure 12: *Radiator diagram. The stationary relative radiator power* $\frac{\Phi}{\Phi_0}$ *as function of the stationary relative flow* $\frac{q}{q_0}$*:* $\Phi_0 = 395$ *W,* $q0 = 17$ *l/h.*

In *(Paulsen and Grundtoft, 1985)* a dynamical thermal radiator model is presented. The model is based on the partial differential equation:

$$C_l \frac{dT}{dt} = c_p \rho q \frac{dT}{dx} - \Phi_{0l} \left(\frac{T - T_a}{60} \right)^{n_1} \tag{31}$$

where T denotes the water (radiator) temperature, T_a the ambient temperature, C_l the heat capacity of water and radiator material per length, and Φ_{0l} denotes the nominal radiator power per length, as in (26). Based on following assumptions:

- No heat transfer in the stream direction of the flow.
- No mix of water in the stream direction of the flow.
- No temperature gradient across the flow.
- No temperature difference between the water and the radiator material.

the idea is to discretize (31) in N sections. The length of each section becomes L/N. Thus, the j'th section is given as:

$$\frac{C}{N} \frac{dT_j}{dt} = c_p \rho q (T_{j-1} - T_j) - \frac{\Phi_0}{N} \left(\frac{T_j - T_a}{60} \right)^{n_1} \tag{32}$$

where C denotes the heat capacity of water and radiator material, and Φ_0 the nominal radiator power. Note that $T_j = T_i$ for $j = 0$, i.e. equal to the water supply temperature. According to *(Paulsen and Grundtoft, 1985)*, $N = 10$ sections is a fair choice. This model is more or less a dynamic version of (26).

3.1.3 Pump model

The central heating system contains two types of active elements: 1) pumps, and 2) thermostatic valves. The hydraulic pressure, produced by an ideal pump, can be described as (see e.g. *(Pfleiderer, 1961)*):

$$\Delta p = p \left(1 - \left(\frac{q}{q_{max}} \right)^2 \right) \tag{33}$$

Using the so called "affinity laws", the pump speed dependency incorporated into (33), yields:

$$\Delta p = p_{max} \left(\left(\frac{n_p}{n_{max}} \right)^2 - \left(\frac{q}{q_{max}} \right)^2 \right) \tag{34}$$

where n_p denotes the actual pump speed. p_{max}, q_{max} and n_{max} depend on the used pump.

3.1.4 Thermostatic valve model

The function of a thermostatic valve is to control the flow into the radiator, and by this means, indirectly the room temperature. The modelling of the thermostatic valve is, from a numerical point of view, a demanding task, as the thermostatic valve is a quite non-linear component. *(Svensson, 1978)* reports dead-times from 0.5 to 17 minutes, time constants from 13 to 60 minutes (quite big), and hysteresis from 0.5 to 2.3°C . Moreover, the thermostatic valve is influenced by the temperature of the bypassing water and the available pressure over the valve. According to *(Danfoss, 1988)*, the working pressure over a valve should be in the range 0.1 – 0.3 Bar. A sketch of a thermostatic valve is shown in Figure 13.

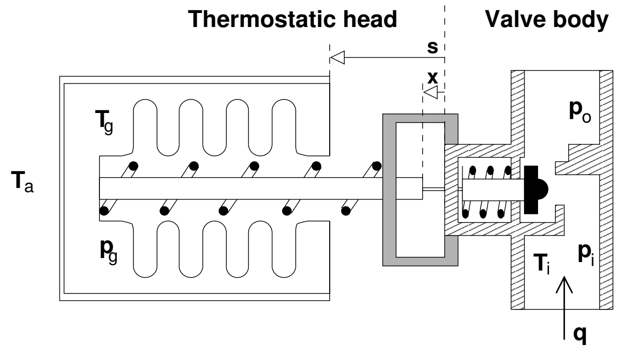

Figure 13: *Schematic drawing of a thermostatic valve (based on saturated vapor).*

As indicated in Figure 13, the thermostatic valve consists of two parts: a thermostatic sensor and a valve body. In *(Gammelby, 1974)*, 4 thermostatic valve types are presented and the above mentioned properties are discussed. It is further concluded that the gas based thermostatic valve is the most advantageous. Hence, based on the considerations above (including *(Gammelby, 1974)*) the following modelling terms are used:

- The dead-time is set to 0 minutes.
- The time constant is set to 15 minutes.
- Influence from the bypassing water temperature and dependency on the working pressure (alias elasticity) are neglected.
- Phenomenas like friction or sticktion (backlash) with respect to the valve piston can be neglected.
- Hysteresis is neglected.

A physical model can now be established. The displacement of the piston is governed by two main forces (the friction force is neglected): 1) the pressure force F_g due to the small gas volume in the thermostatic valve – the "sensor" and 2) the spring/pod force F_s. First, the gas in the sensor is assumed to be an ideal gas, thus:

$$\frac{p_g V_g}{T_g} = K_g \tag{35}$$

where K_g denotes some gas constant, and V_g the volume of the gas. The volume V_g has an upper and a lower bound, due to the physical constraint on the valve spindle displacement x. It can be modelled as:

$$V_g = -A_g(x - x_0 + s) + V_0 \tag{36}$$

where V_0 is the gas volume at $x = x_0 - s$, and A_g denotes the sectional area of the sensor pod. s is related to the displacement of the valve spindle and the set point temperature (when the thermostatic head is turned, s is changed). The forces must satisfy Newton's second law (assuming the spring/pod to be linear):

$$M_p \frac{d^2x}{dt^2} = -F_g + F_s = -p_g V_g - k_s(x - x_s + s) - k_p(s - s_s) \approx 0 \tag{37}$$

where k_s denotes the combined spring and pod constant and $x - x_s + s$ the

displacement in the spring from the non tightened state ($x - x_s + s = 0$). Assuming that $M_p \frac{d^2x}{dt^2} \approx 0$ and substitution of (35) and (36) into (37), yield:

$$A_g K_g T_g = -k_s(x - x_s + s)(-A_g(x - x_0 + s) + V_0) \tag{38}$$

which is a stationary description of the relation between the sensor temperature T_g and the valve spindle position x. Assuming that $A_g(x - x_0 + s) \ll V_0$, it can be seen that, x decreases when T_g increases (the valve is closing). Therefore, it can be assumed that, the relation between the room temperature and the valve opening is approximately negative proportional. Equation (38) contains 6 constant – of which some might be difficult to determine.

In the data sheets (see e.g.*(Danfoss, 1988)*) the valve constant K_v is listed as function of the P-band temperature X_p (a relative temperature) at a pressure drop of 1 Bar (over the valve):

$$K_v(X_p) = q/\sqrt{\Delta p} \equiv q_{1Bar} \tag{39}$$

The P-band temperature is defined as:

$$X_p = T_{set} + 2 - T_g \tag{40}$$

where T_{set} denotes the set-point temperature of thermostatic valve. When $X_p = 0$ the valve should be closed. In Table 1, characteristic data for the used[4] thermostatic valve are listed.

x_p	0.5	1	1.5	2.0	K_{vs}	K
q_{1Bar}	0.22	0.40	0.55	0.65	0.85	m^3/h
K_v	0.22	0.40	0.55	0.65	0.85	$m^3/h/Bar^{0.5}$
$R_v = \frac{1}{K_v^2}$	20.7	6.25	3.31	2.37	1.38	$Bar{\cdot}h^2/m^6$

Table 1: *RA-FN 15 valve data. The flow at different P-band temperatures at a pressure drop $\Delta p = 1$ Bar over the valve.*

The valve flows, listed in Table 1, are at 1 Bar valve pressure drop. The operational pressure drop should be in the area of 0.1 to 0.3 Bar, i.e. at $\frac{1}{\sqrt{0.3}} \sim 1.8$ to $\frac{1}{\sqrt{0.1}} \sim 3.2$ times smaller flows than listed in the Table 1. It

[4] applied in the radiator terminal

can be observed that, compared with the flows in (3) and (4), the valve flows at the operational pressures are much bigger. Thus, to be able to satisfy the smaller flow demand the valve would have to be "more closed".

A more profound description of a thermostatic valve model is to be published in *(Hansen et al., 1997)*. The basic ideas of the paper are:

1. to describe the nonlinear relation between the P-band temperature X_p and the valve constant by (as shown in e.g. Table 1):

$$\mathrm{K}_v(X_p) = a \tanh(b\, X_p) \tag{41}$$

where a and b are two constant and $X_p = T_{set} + 2 - T_g$.

2. to model the relation between the surrounding room temperature T_r (of the valve) and the gas sensor temperature T_g by the dynamic model:

$$\frac{dT_g}{dt} = \frac{1}{\tau}(T_r - T_g) \tag{42}$$

where τ denotes the time constant of the valve. X_p and T_g are related as in (40).

The constants in this thermostatic valve model has been estimated on real measurement data from the central heating system (described in Section 2.1). It is furthermore shown in *(Hansen et al., 1997)* to have a good modelling performance.

As the valve only contains a small amount of water (compared with a pipe), the hydraulic valve impedance L_v is approximately zero. The hydraulic valve resistance R_v depends on the P-band temperature. Using (41), the hydraulic valve resistance can be calculated as:

$$\mathrm{R}_v(X_p) = \frac{\Delta p}{q^2} = \frac{1}{(a \tanh(b\, X_p))^2} \tag{43}$$

3.1.5 The hydraulic central heating system model

As described above the thermostatic valve is just a variable (nonlinear) hydraulic resistance. Hence, the central heating system sketched in Figure 9,

can be modelled by a second order nonlinear model.

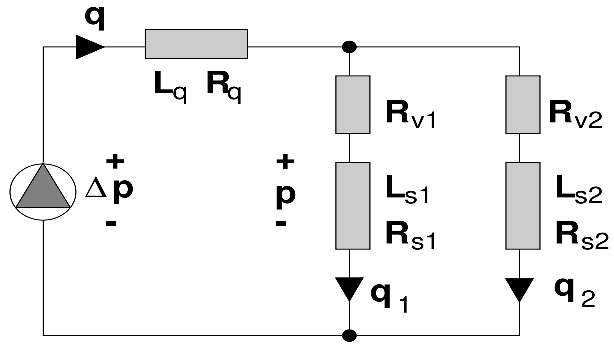

Figure 14: *Hydraulic lumped model of the central heating system setup.*

Based on Figure 14 the following equations are formulated:

$$\Delta p = L_q \frac{dq}{dt} + R_q(q)q + p \tag{44}$$

$$p = L_{s1}\frac{dq_1}{dt} + R_{s1}(q_1)q_1 + R_{v1}(X_p)q_1^2 \tag{45}$$

$$p = L_{s2}\frac{dq_2}{dt} + R_{s2}(q_2)q_2 + R_{v2}(X_p)q_2^2 \tag{46}$$

$$q = q_1 + q_2 \tag{47}$$

For convenience the flow dependency in the hydraulic resistances is dropped. The set of equations above can be reduced to the following coupled nonlinear first order differential equations:

$$\begin{aligned} LL\frac{dq_1}{dt} &= L_{s2}\Delta p - (R_q L_{s2} + (R_{s1} + R_{v1}(X_p)q_1)(L_q + L_{s2}))q_1 \\ &\quad +(R_{s2}L_q - R_q L_{s2} + R_{v2}(X_p)L_q q_2)q_2 \qquad (48) \\ LL\frac{dq_2}{dt} &= L_{s1}\Delta p - (R_q L_{s1} + (R_{s2} + R_{v2}(X_p)q_2)(L_q + L_{s1}))q_2 \end{aligned}$$

$$+(R_{s1}L_q - R_qL_{s1} + R_{v1}(X_p)L_qq_1)q_1 \quad (49)$$

where $LL = L_qL_{s1} + L_qL_{s2} + L_{s1}L_{s2}$. Δp depends on the pump speed n and the flow q_1+q_2 as described in (34). This model can be used as a model of the hydraulic part of the central heating system.

3.2 Model of the test house

As shown e.g. in Figure 5, the house contains three rooms: the control room B, and the two test rooms An and As of 60 m^2, 30 m^2, and 30 m^2, respectively. Room B is not the main target of the modelling, as it contains the heating unit and the data acquisition system. The modelling of room B will, however, be discussed later.

3.2.1 Model of the test rooms

The heat from the central heating system goes through test rooms to the environment. To obtain a simple lumped model of the test rooms, the following assumptions are made:

- The air in a room is perfectly mixed, which makes it possible to describe the room temperature by a single state.
- The floor consists of a sandwich structure as described in Section 2.2. Only the upper concrete layer is assumed to interact with the room air temperature. This assumption is justified by the non-ventilated crawl space and the insulation layer.
- Negligible heat exchanges through the ceiling. This can be justified by the two facts: 1) the ceiling is quite well insulated, and 2) the temperature level in the roof-storey (the office space) is about the same as in the ground floor.
- The thermal heat capacity of the outer wall and the inner walls are negligible.
- The northern and southern ambient temperature are identical, i.e. $T_{am} = T_n = T_s$.
- No influence from windy or rainy weather.

- All heat transfer by radiation will be neglected, except for the solar radiation.

With these assumptions a thermal network model, of e.g. room An, can be formulated, as illustrated in Figure 15.

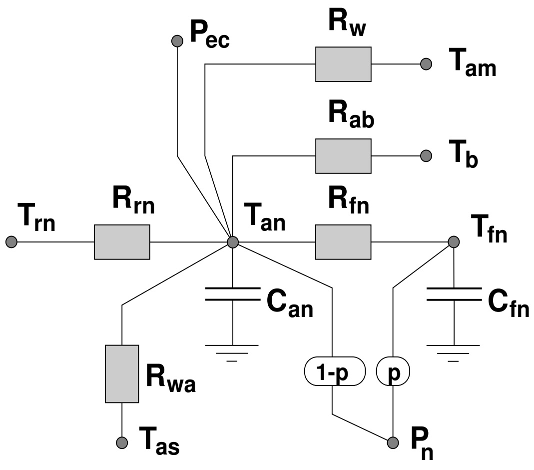

Figure 15: *Thermal network equivalent model of room An.*

The R's in Figure 15 denote the thermal resistances between two temperatures and the C's denote the thermal heat capacities associated with a particular temperature. The model states and inputs of the An-room model are:

- The two states: T_{an} and T_{fn}, the air temperature in room An and the temperature of the floor in room An, respectively. T_{an} represents the two measured temperatures: T_{nw} and T_{ne}.
- The state T_{rn}, the mean temperature of the center of the radiator in box 2 and the input T_{am}, the ambient temperature (outside temperature).
- The input T_b, the temperature in room B and the state T_{as}, the temperature in room As.
- The input P_{ec}, the heat input from the electric cooker.

- The input P_n, denotes the heat input from the solar radiation through the northern windows. The heat input P from the solar radiation is equal to the solar radiation I passing the effective window area[5] A, i.e. $P = I \cdot A$. $1-p$ and p denote fractions describing the amount of solar radiation heat, that heats the air and the floor, respectively. In *(Madsen et al., 1990)*, p is reported to be close to zero.

One of the assumptions in the modelling of the test room models (room A model) is that the northern and southern ambient temperature are identical. The same assumption cannot be made on the solar radiation. Therefore, the input heat from the solar radiation is divided into P_n and P_s (northern and southern radiation heat inputs). The northern radiation heat input is due to diffuse solar radiation, whereas the southern is due to both diffuse and direct solar radiation.

Based on Figure 15 the following second order model can be formulated for the heat transfer in room An:

$$
\begin{aligned}
C_{an}\frac{dT_{an}}{dt} &= \frac{1}{R_{rn}}(T_{rn}-T_{an})^{n_1} + \frac{1}{R_{fn}}(T_{fn}-T_{an}) \\
&\quad + \frac{1}{R_{wa}}(T_{as}-T_{an}) + \frac{1}{R_{w}}(T_{am}-T_{an}) \\
&\quad + \frac{1}{R_{ab}}(T_{b}-T_{an}) + (1-p)P_n + P_{ec} \qquad (50) \\
C_{fn}\frac{dT_{fn}}{dt} &= \frac{1}{R_{fn}}(T_{an}-T_{fn}) + P_n \qquad (51)
\end{aligned}
$$

where n_1 denotes the radiator exponent as described in the previous section. An identical second order model can be formulated for the heat transfer room As, except for the P_{ec} input, as the electric cooker is placed to room An. Thus, the heat transfer in the A-rooms are described by a set of 4 coupled first order differential equations – with the 4 states: T_{an}, T_{fn}, T_{as} and T_{fs}, and the 7 inputs: $T_{rn}, T_{rs}, T_b, T_{am}, P_n, P_s$ and P_{ec}.

[5] the effective window area is a function of sun position

It should be noted that in the interpretation of Figure 15 the one exponent has been used and modified as follows:

$$
\begin{aligned}
\Phi &= \Phi_0\left(\frac{\Delta T_m}{\Delta T_{ma}}\right)^{n_1} \qquad (52) \\
&= \frac{\Phi_0}{(\Delta T_{ma})^{n_1}}(\Delta T_m)^{n_1} \qquad (53) \\
&= \frac{1}{R_{rn}}(T_{rn}-T_{an})^{n_1} \qquad (54)
\end{aligned}
$$

where $\frac{1}{R_{rn}} = \frac{\Phi_0}{(\Delta T_{ma})^{n_1}}$ and $\Delta T_m = \frac{1}{2}(T_i + T_o) - Ta \equiv T_{rn} - T_{an}$.

3.2.2 Model of the control room

So far the test rooms were considered. Room B is slightly more difficult to model, due to uncertainty on the heat input from the heating unit and all the data acquisition instruments (computer, etc.). The thermal heat capacity of room B is equal to the thermal heat capacity of room A (see Section 2.2). For the considered setup of the experiment, it is assumed that the air temperature in room B will be dominated by its floor temperature. Therefore it is reasonable to assume that, the air temperature in room B can be described by a single first order differential equation:

$$
\begin{aligned}
C_b\frac{dT_b}{dt} &= \frac{1}{R_{wb}}(T_{am}-T_b) + \frac{1}{R_{ab}}(T_{an}-T_b) \\
&\quad + \frac{1}{R_{ab}}(T_{as}-T_b) + P_{load} \qquad (55)
\end{aligned}
$$

where C_b denotes the total heat capacity of the air and of the concrete flags in room B, and P_{load} denotes the heat input from the heating unit, computer etc.

It is possible to increase the energy loss in room B, if the energy loss of house is found to be too small. Room B is equipped with a air ventilation system. Using this system, to increase the energy loss in room B, a second order model of room B should be used.

3.3 Interconnection between heating system and room

The interconnection between the central heating system and the test room is realized through the functionality of the radiator and the thermostatic valve. For example, if the radiator feeds the room with more heat than needed, the thermostatic valve decreases the water flow. Due to this action the heat from the radiator is adjusted. Hence, the system consisting of thermostatic valve, radiator and room conform a controller loop with the thermostatic valve as controller.

The hydraulic heating system model, (48) and (49), and the the thermal room model, (50) and (51), can be combined using the thermostatic valve models, (41) and (42) and the dynamic radiator model, (32), with an adequate number of sections. Thus, the model of the test rooms with the heating system constists of $2 \times (4 + N)$ first order differential equations, where N denotes the number of sections in the radiator.

4 Design of the input signals

As mentioned in the introduction, the heat transfer in the experiment is controlled by two kinds of inputs: 1) the controllable and 2) the climatic inputs. This section deals with the design the three controllable inputs: 1) pump speed, 2) supply temperature and 3) the electric cooker.

4.1 System analysis

Some knowledge about the system must be available before the input signals can be designed. The required knowledge is mainly about the time constants of the system and suitable input levels providing a reasonable range of the

system states.

The time constants are found through a linearization of the model. The most interesting time constants are those of the room temperature T_{an} and the floor temperature T_{fn} (dito room As). The time constants become:

$$\tau_{an} = C_{an} \frac{1}{\frac{1}{R_{rn}} + \frac{1}{R_{fn}} + \frac{1}{R_{wa}} + \frac{1}{R_w} + \frac{1}{R_{ab}}} \tag{56}$$

$$\tau_{fn} = C_{fn} R_{fn} \tag{57}$$

These are the dominating time constants, see *(Madsen et al., 1990)*. In Table 2 a set of thermal resistances and thermal capacities are shown. They have been calculated based on the informations gathered in Section 2.2. R_{rn} is calculated at $\Delta T_{ma} = 35$ K, $n_1 = 1.25$ and $\Phi_0 = 395$ W.

Parameter	Calculated value	Unit
C_{an}	79.0	KJ/K
C_{fn}	4.35	MJ/K
R_{rn}	$216 \cdot 10^{-3}$	W/K
R_{fn}	$44.4 \cdot 10^{-3}$	W/K
R_{wa}	$211 \cdot 10^{-3}$	W/K
R_w	$263 \cdot 10^{-3}$	W/K

Table 2: *Assumed values for the thermal resistances and the thermal capacities.*

Using the parameter values in Table 2, the time constants τ_{an} and τ_{fn} become approximately 37 minutes and 54 hours, respectively. It should be noted that these values are based on simplified circumstances, i.e. they represent “a good” guess on the “real” values. In *(Hansen et al., 1997)* the time constant of thermostatic valve is estimated to 13 minutes. Thus, the thermostatic valve can control the room temperature, as the bandwidth of the thermostatic valve is larger than the bandwidth of the room temperature.

4.2 Input design

The idea with the input signal design is to design a signal, which excites the system in order to extract information of the dynamical properties of the system.

A Pseudo Random Binary Signal (abbreviated as PRBS) is used as the controllable input signal. The PRBS-signal alternates (the random issue) between two levels (the binary issue). A detailed description of the PRBS-signal is given in *(Godfrey, 1980)*. A PRBS-sequence is designed by two parameters: 1) the number of states N_{prbs} in the shift register and 2) the fundamental time period T_{prbs} (the shortest period of a constant signal level).

In the analysis above two time constants were claimed to dominate the thermal dynamics of the test house: a small time constant of the room and a large time constant of the floor. The heat unit contains 80 litters of water, which makes it thermally heavy. Hence, the supply temperature will be used to excite the system in the frequency domain related to the large time constant, while the pump pressure will be used to excite the system in the frequency domain related to the small time constant.

The assumed thermal resistances shown in Table 2 are subjected to some uncertainty. Meanwhile, this uncertainty can more or less be covered in the design of the input signals. As the PRBS-signal can be viewed as a cascade of step inputs, the fundamental time period T_{prbs} of the PRBS-signal should be selected smaller than the expected time constant. The number of states N_{prbs} in the shift register should then be selected such that the expected time constant is included in the interval from T_{prbs} to $N_{prbs} \cdot T_{prbs}$. The two interval limits T_{prbs} and $N_{prbs} \cdot T_{prbs}$ can be adjusted in order to reflect the uncertainty on the expected time constant.

The PRBS-signals for the set point of the supply temperature and the pump speed reference are chosen as shown in Table 3. R_{fn} is the thermal resistance with the largest uncertainty. As τ_{fn} is more influenced by R_{fn} than τ_{an}, a larger interval on τ_{fn} is necessary.

As described in Section 2.2 an additional heat input was placed in the northern test room (room An). This extra heat input is denoted as electric cooker. Due to the windows the solar radiation will influence both test rooms. Of course the influence will be strongest in the southern room As (room As). The purpose of the electric cooker is to decouple the solar radiation heat input. As shown in Table 3 the fundamental time period of the electric cooker heat input is chosen not to match the diurnal solar radiation.

Input signal type	T_{prbs}	N_{prbs}
Supply temperature	30 hours	6
Pump speed	20 minutes	4
Electric cooker	9 hours	3

Table 3: PRBS-signal design parameters.

An other input design approach is described in *(Sadegh et al., 1997)*. This paper is concerned with problem of estimating a set of unknown parameters or detecting parametric changes in the dynamic system consisting of the low energy test house and the water based central heating system.

5 Summary

The experimental setup consisting of a water based central heating system and a low energy test house has been described. PRBS-signals have been used for the controllable input signals in the planned experiment. In order to design the PRBS-signals appropriately, a dynamic model of the heat transfer in the experimental setup is established based on hydraulic and thermo dynamic considerations. The modelling is focussed on dynamic models of the following "components" in the experimental setup: pipe, radiator, pump, thermostatic valve and room.

6 Acknowledgements

This work conforms a part of my Ph.D. study, which is financed by Grundfos A/S and Academy of the Technical Sciences in Denmark.

First I want to acknowledge my four supervisors: Niels Bidstrup from Grundfos A/S, Jan Holst from Department of Mathematical Statistics at the University of Lund in Sweden, Henrik Madsen from Department of Mathematical Modelling and Pierré Vadstrup from Grundfos A/S, for fruitful discussions and for their willingness to answer all kinds of questions.

Moreover I want to thank the people at the Department of Buildings and Energy for their cooperation, especially Bjarne Saxhof and Jørgen M. Schultz.

References

Aggerholm, S. (1983). *Simulering af varmeanlæg.* PhD thesis, Laboratoriet for Varme- og Klimateknik, the Technical University of Denmark.

Becher, P. (1972). *Varme og ventilation, Bind 2.* Teknisk Forlag.

Danfoss (1988). *Radiatortermostat/Ventilhuse, RA 2000/RA-FN og RA-G.* Danfoss A/S, vd.51.a5.01 edition.

Data Translation (1995). *How to use DT VEE.* Data Translation, 1 edition.

Fox, R. W. and McDonald, A. T. (1985). *Introduction to Fluid Mechanics.* John Wiley & Sons.

Gammelby, J. (1974). Heizkörperthermostate. grundsätze und eigenschaften. *Danfoss Journal*, 3.

Godfrey, K. R. (1980). Correlations methods. *Automatica*, 16:527–534.

Hallgreen, L. and Paulsen, O. (1987). Lavtemperatur varmeanlæg – dimensionering af radiatorer. Technical report, Teknologisk Institut, Varmeteknik.

Hansen, F. M. (1985). *Varmetilførsel til bygninger (Estimation og optimal regulering).* Master's thesis, IMSOR, DTH. Nr. 2/85.

Hansen, L. H., Bidstrup, N., Madsen, H., Vadstrup, P., and Holst, J. (1995). A hydraulic simulink model of the heating system in a single family house. In Langemyr, L., editor, *Nordic Matlab Conference '95*, volume II, pages 114–118. Computer Solutions Europe AB, Sweden.

Hansen, L. H., Madsen, H., Holst, J., Bidstrup, N., and Vadstrup, P. (1997). A dynamic nonlinear model of a thermostatic valve. In *Clima 2000.*

Johansen, J., Paulsen, O., Svenningsen, N., and Øhrgaard, P. (1979). Vandvarmeovnens varmeydelser. Technical report, Varme- og Installationsteknik, Teknologisk Institut. Rapport 2.

Madsen, H., Melgaard, H., and Holst, J. (1990). Identification of building performance parameters. In Bloem, J. J., editor, *Workshop on Advanced Identification Tools in Solar Energy Research*, Non Nuclear Energy, pages 37–60. Commission of the European Communities, DG XII.

Paulsen, O. and Grundtoft, S. (1985). Dynamisk afprøvning af små varmecentraler. Technical report, Teknologisk Institut, Jydsk Teknologisk Institut.

Pfleiderer, C. (1961). *Die Kreiselpumpen für Flussigkeiten und Gase.* Springer-Verlag.

Rasmussen, N. H. and Saxhof, B. (1982). Simultaneous testing of heating systems (report no. 128). Technical report, Thermal Insulation Laboratory, DTU.

Sadegh, P., Hansen, L. H., Madsen, H., and Holst, J. (1997). Maxmin input design for linear dynamic systems. *Journal of Information & Optimization Sciences*. To be published.

Svensson, A. (1978). Radiatortermostatventilors funktion, m78:4. Technical report, The national Swedish institute for Building Research. Lägesrapport.
In Eng.: Functionality of Thermostatic Radiator Valves.

Thor Eura (1990). *Thor Riffel radiatorer*. Northor A/S, 1 edition.

Weber, A. P. (1970). *Die Warmwasserheizung*. R. Oldenbourg, München.

Zoebl, H. and Kruschik, J. (1978). *Strömung durch Rohre und Ventile*. Springer-Verlag.

OTHER IMM TECHNICAL REPORTS 1996.

Lund, K., O.B.G. Madsen og J.M. Rygaard:
Vehicle routing problems with varying degrees of dynamism, revised edition.
Nr. 1/1996. 22 pp.

Albertsen, N.C., S. Christiansen, K. Pontoppidan og S.B. Sørensen:
Mathematical treatment of an adjustable surface formed by a fabric of interwoven flexible wires.
Nr. 2/1996. 31 pp.

Sadegh, P.:
Constrained optimization via stochastic approximation with a simultaneous perturbation gradient approximation.
Nr. 3/1996. 10 pp.

Hansen, A.P. og N.K. Poulsen:
Tracking keeping systems with predictive control.
Nr. 4/1996. 27 pp.

Barker, V.A.:
Computing connection coefficient.
Nr. 5/1996. 16 pp.

Thyregod, P.:
Statistisk vurdering af analysemateriale.
Nr. 6/1996. 45 pp.

Kulikov, G.Y. og P.G. Thomsen:
Convergence and implementation of implicit runge-kutta methods for DAEs.
Nr. 7/1996. 29 pp.

Kulikov, G.Y.:
Convergence results for iterative implicit multistep methods with fixed step size.
Nr. 8/1996. 37 pp.

Christiansen, S. og R.E. Kleinman:
On a misconception involving point collocation and the rayleigh hypothesis (II).
Nr. 9/1996. 28 pp.

Hansen, A.D. og N.K. Poulsen:
Predictive control relevant prefiltering.

Nr. 10/1996. 40 pp.
Jørgensen, C.,O.B.G. Madsen og H. Ravn:
Parallel implementations of optimal feedback solutions of a discrete time stochastic problem.
Nr. 11/1996. 11 pp.
Jørgensen, C. og H.F. Ravn:
Optimal feedback solution: a constrained stochastic one-storage model.
Nr. 12/1996. 26 pp.
Kulikov, G.Y.:
Modern theory of symmetric one-step methods for ODEs.
Nr. 13/1996. 17 pp.
Albertsen, N.C.:
Diffraction by a quarterplane of the field from a halfwave dipole.
Nr. 14/1996. 18 pp.
Ekblom, H. og H.B. Nielsen.:
A comparison of eigth algorithms for computing M-Estimates.
Nr. 15/1996. 14 pp.
Christiansen, S.:
On the elastostatic significance of four boundary integrals involving biharmonic functions.
Nr. 16/1996. 13 pp.
Bendtsen, C. og O. Stauning:
FADBAD, a flexible C++ package for automatic differentiation.
Nr. 17/1996. 33 pp.
Stauning, O.:
Enclosing solutions of ordinary differential equations.
Nr. 18/1996. 42 pp.
Caprani, O., K. Madsen og O. Stauning:
Enclosing solutions of integral equations.
Nr. 19/1996. 19 pp.
Hansen, L.H.:
Dynamic analysis of a low energy test house and a central heating system.
Nr. 20/1996. 41 pp.